

Universal spin excitations in fluctuating stripe phases

Matthias Vojta¹, Thomas Vojta² & Ribhu K. Kaul^{1,3}

¹*Institut für Theorie der Kondensierten Materie, Universität Karlsruhe, 76128
Karlsruhe, Germany*

²*Physics Department, University of Missouri, Rolla, MO 65409, USA*

³*Physics Department, Duke University, Science Drive, Durham, NC 27708, USA*

A key challenge in the field of high- T_c superconductivity is to separate universal from non-universal material properties. For spin fluctuations, believed to be the glue that binds the Cooper pairs, this issue is controversial: early neutron scattering experiments had established the existence of a “resonance peak”, corresponding to a spin collective mode at the antiferromagnetic wavevector, for certain cuprate families,^{1–3} while in others stripe-like spin and charge modulations were detected instead.^{4–7} However, recent more detailed measurements^{8–13} point toward a universal spin excitation spectrum at intermediate energies¹⁴ for all cuprate families, namely an “hour-glass” spectrum with a high-intensity peak at the antiferromagnetic wavevector and both downward and upward dispersing branches of excitations. Here we demonstrate that these spectra can be consistently explained in a theoretical framework of fluctuating stripes, thus providing a universal description of the various experimental observations. While weakly fluctuating stripe domains are consistent with the data on $\text{La}_{2-x}\text{Sr}_x\text{CuO}_4$ (LSCO) and $\text{La}_{2-x}\text{Ba}_x\text{CuO}_4$ (LBCO), a mixture of stripe and checkerboard structures, leading to nearly isotropic two-dimensional magnetism, is required to explain the experimental data^{9,10} on nearly optimally doped $\text{YBa}_2\text{Cu}_3\text{O}_{6+\delta}$ (YBCO). Our calculations unify the spin dynamics of static and fluctuating stripe phases, and the results suggest that stripe-like charge modulations are a universal phenomenon of all cuprates.

The discovery of spin- and charge-density waves, commonly referred to as stripes, in the LSCO family of cuprate superconductors dates back to the mid-nineties, but was considered to be special for this class of compounds. This view has been challenged by a series of new experiments: (i) Signatures of charge order, likely pinned by impurities, have been observed also in scanning tunnelling microscopy (STM) experiments^{15,16} on $\text{Bi}_2\text{Sr}_2\text{CaCu}_2\text{O}_{8+\delta}$ and $\text{Ca}_{2-x}\text{Na}_x\text{CuO}_2\text{Cl}_2$. (ii) Inelastic neutron scattering⁸⁻¹³ over a larger range of energies have revealed remarkably similar spin excitation spectra in the LSCO/LBCO and YBCO families. However, a unified theoretical description is lacking, and different approaches have been employed: the spin excitations⁸ in $\text{La}_{15/8}\text{Ba}_{1/8}\text{CuO}_4$ are well explained within a framework of static stripes,¹⁷⁻¹⁹ where weak magnetic order exists on top of a bond-ordered (i.e. dimerized) background.^{18,19} In contrast, neutron scattering in YBCO was modelled using RPA-type calculations^{20,21} which, however, rely on details of the band structure and are not able to describe ordered states (e.g. in LBCO). A key question is whether the neutron scattering data on YBCO can be understood in a stripe picture as well – as no static order has been detected, stripes have to be fluctuating in space and time here. Controversial experimental viewpoints on this have been put forward.^{6,9,14} The purpose of this letter is to show that *fluctuating stripes*²²⁻²⁴ lead to spin excitations very similar to those observed in the experiments, thus providing a unified account of the universal collective mode dynamics in the cuprates.

We employ a phenomenological Landau theory of coupled spin and charge fluctuations.²⁵ The primary input is that the spin incommensurabilities are driven by inhomogeneities in the charge sector; this is supported, e.g., by experiments on stripe-ordered LSCO, where the charge order sets in at a higher temperature than the spin order. On a microscopic scale, the influence of the charge order on the spin sector can be understood as spatial modulations of both spin densities and magnetic couplings, as in Refs. 16,17. The goal of our work is to describe well-defined collective modes in

strongly correlated materials, hence we neglect the continuum of single-particle excitations and the associated collective mode damping.

The full action of our Landau theory has the form $S = S_\phi + S_\psi + S_{x,y}$, with the partition function $Z = \int D\psi \exp(-S_\psi) \int D\phi \exp(-S_\phi - S_{x,y})$, where S_ϕ (S_ψ) describe the spin (charge) fluctuations, and $S_{x,y}$ couples the two; see the Supplementary Information for details. We assume a dominant antiferromagnetic interaction, and so employ a lattice ϕ^4 theory for the spin fluctuations at the *commensurate* wavevector $\mathbf{Q} = (\pi, \pi)$. The real order parameter ϕ_j and the spin \mathbf{S}_j on the sites j of the square lattice of copper atoms are related through $\mathbf{S}_j \sim \exp(i \mathbf{Q} \cdot \mathbf{r}_j) \phi_j$. Turning to the charge sector, we note that microscopic calculations have indicated a tendency towards states with stripe-like charge ordering,^{26,27} but states with two-dimensional (2d) “checkerboard” modulations closely compete in energy.^{28,29} We employ *two* complex order parameter fields $\psi_{x,y}(\mathbf{r}, \tau)$ which measure the amplitude of horizontal and vertical stripe order at wavevectors $\mathbf{K}_{x,y}$. Checkerboard order then implies *both* ψ_x and ψ_y non-zero. In a situation with fluctuating charge order, the balance between stripes and checkerboard (which depends on microscopic details²⁸) is controlled by a repulsion or attraction between ψ_x and ψ_y . The complex phase of $\psi_{x,y}$ represents the sliding degree of freedom of the density wave and distinguishes between bond- and site-centered stripes. In our simulations we concentrate on $\mathbf{K}_x = (\pi/2, 0)$ and $\mathbf{K}_y = (0, \pi/2)$, i.e., a charge modulation period of 4 lattice spacings; modulations at these wavevectors have been observed both in neutron scattering^{4–7} and STM^{15,16}, in particular near doping 1/8 where stripe order is most robust. The real field $Q_x(\mathbf{r}) = \text{Re } \psi_x(\mathbf{r}) \exp(i \mathbf{K}_x \cdot \mathbf{r})$ (similarly for Q_y) measures the modulation of both the charge density (for \mathbf{r} on sites) and bond order (i.e., kinetic energy or pairing amplitude, for \mathbf{r} on bonds). The all-important couplings between spin and charge fluctuations have to be of the form $\lambda Q \phi^2$ due to the underlying SU(2) spin symmetry. These terms implement the correlation between the charge densities and both

the amplitudes of the spin fluctuations and the spatial modulations of the exchange constants (see Supplementary Figure 1).

If $\psi_{x,y}(\mathbf{r}, \tau)$ is constant in space and time, then the action $S_\phi + S_{x,y}$ is a theory for magnetic modes in a background of static charge order. For sufficiently large λ couplings, the minimum energy of the spin fluctuations will be shifted away from (π, π) to the incommensurate wavevector dictated by the charge order (this is a non-perturbative effect!), with the spin order remaining collinear. Results for the spin fluctuation spectrum in the presence of static stripes have been reported in Ref. 25, and are in excellent agreement with experimental data on LBCO.⁸

How are the spin excitations modified when the stripes start to fluctuate? To answer this, we focus on the charge theory S_ψ in its disordered phase, and study its influence on the spin dynamics. To simplify the treatment of $(S_\phi + S_\psi + S_{x,y})$, we assume that fluctuations in the charge sector are slow compared to those in the spin sector. (The fact that, in stripe-ordered compounds, the charge sector orders *before* the spin sector upon lowering temperature, implies slower charge fluctuations.) We are lead to an adiabatic (Born-Oppenheimer) approximation for the coupled dynamics, which allows us to treat the charge fluctuations by *classical* lattice Monte Carlo (MC) simulations. For each configuration of the charge order parameters $\psi_{x,y}$, the remaining theory $S_\phi + S_{x,y}$ (at the Gaussian level) is quadratic in the ϕ fields and can be diagonalized numerically. The concrete form of the model S_ψ turns out to be decisive: it will, e.g., determine the importance of amplitude and phase fluctuations of the stripe order. Note that S_ψ has to capture the complicated physics of a strongly correlated system on the lattice scale, see Supplementary Information for details. Among the terms in S_ψ , most important is $(\nu |\psi_x|^2 |\psi_y|^2)$ which regulates the repulsion or attraction between horizontal and vertical stripes; note that condensing the charge order leads to a stripe (checkerboard) phase for $\nu > 0$ ($\nu < 0$). Typical snapshots of the two charge order

parameters $\psi_{x,y}$ and the resulting charge configuration, for different values of the interaction v , are shown in Fig. 1.

Let us now discuss our results for the zero-temperature dynamic spin susceptibility, $\chi''(\mathbf{q},\omega) = \langle \mathbf{S}(\mathbf{q},\omega) \mathbf{S}(-\mathbf{q},-\omega) \rangle$, that is measured in inelastic neutron scattering. Starting from ordered stripes,²⁵ we found that spatial fluctuations of the amplitude of ψ rather quickly destroy the low-energy incommensurate spin excitations; for a standard ψ^4 theory this happens already within the ordered phase. In contrast, the spin sector turns out to be less sensitive to phase fluctuations of the stripe order. Microscopically, this means that incommensurate spin correlations require well-formed stripe segments with a length of at least 10 lattice spacings. We have therefore focussed on versions of S_ψ with small amplitude fluctuations, and carried out large-scale simulations for various couplings and correlation lengths of the $\psi_{x,y}$.

Sample results for the dynamic susceptibility, corresponding to the situations in Fig. 1, are shown in Fig. 2. The right panels show that a common feature of all spectra is a strong “resonance” peak at (π,π) and energy E_{res} . For small charge correlation length ξ there is only an upward dispersing branch; with increasing ξ the downward dispersing branch becomes more pronounced (see Supplementary Figure 2). Our calculations thus show that the “spin gap”, i.e., the low-energy range with very small intensity, increases due to stripe fluctuations.

We have studied in detail the crossover from a strictly “stripy” situation with a strong repulsion between ψ_x and ψ_y (Figs. 1a and 2a) to a 2d checkerboard regime with attraction between ψ_x and ψ_y (Figs. 1c and 2c). Significant differences occur in the lower branch (left panels of Fig. 2). For large domains of horizontal or vertical stripe order, Fig. 2a, well-defined peaks occur along (q_x,π) and (π,q_y) , as observed in LBCO. Interestingly, with increasing volume fraction of checkerboard domain walls, Fig. 2b, the spin excitations are both smeared and enhanced along the q-space diagonals,

resulting in a quasi-2d dispersion of the downward branch - this is strikingly similar to experimental data^{9,10} on YBCO near optimal doping. Finally, in a checkerboard regime the low-energy spin excitations occur along the diagonals (Fig. 2c). Based on these results and STM data¹⁶ we predict that such a neutron scattering response should be observable in $\text{Ca}_{2-x}\text{Na}_x\text{CuO}_2\text{Cl}_2$.

The q-space structure of the upward dispersing branch (middle panels of Fig. 2) changes less from the stripe to the checkerboard regime. It is strongly anisotropic only in the stripy situation of Fig. 2a where it resembles the spectrum of two-leg ladders – here a prominent 45-degree rotation in q-space is visible in the high-intensity peaks when going from $E < E_{\text{res}}$ to $E > E_{\text{res}}$. Focussing on the right panels of Fig. 2, we further observe that larger checkerboard regions tend to suppress the upper branch right above the resonance peak, it re-appears only at somewhat higher energies. This is in remarkable agreement with neutron data on $\text{YBCO}_{6.6}$,¹³ and can be easily understood: For perfect checkerboard order the low and high-energy fluctuations are separated by a large gap,²⁵ and our simulations interpolate between stripes and checkerboard. (An alternative interpretation of the data of Ref. 13 within RPA is in Ref. 21.)

To model de-twinned $\text{YBCO}_{6.85}$,⁹ it is necessary to include an in-plane anisotropy to account for the orthorhombic distortions. Assuming the anisotropy to be small, it will mainly influence the low-energy charge fluctuations. We have therefore carried out simulations where the ψ_x and ψ_y charge order parameters had different mass and/or different gradient terms (i.e. velocities). Sample results for the downward dispersing branch are shown in Fig. 3, which are in reasonable agreement with the data of Hinkov *et al.*⁹ The anisotropy decreases at higher energies (not shown).

In conclusion, we have determined the spin excitation spectrum in the presence of fluctuating stripe charge order. We obtain incommensurate spin excitations, consistent with available experimental data on cuprate superconductors, provided that (i) charge

order fluctuates predominantly in phase rather than in amplitude, and (ii) the charge correlation length is at least 10 lattice spacings. (Assuming a collective mode velocity of 50 meV this roughly translates into THz fluctuation frequencies.) In addition, we found that an increasing volume fraction of stripe domain walls with checkerboard structure leads to quasi-2d spin dynamics as observed in YBCO. We predict that the spin fluctuations in $\text{Ca}_{2-x}\text{Na}_x\text{CuO}_2\text{Cl}_2$, with a checkerboard charge order, will be pronounced along the q-space diagonals, with a clear gap between the lower and upper excitation branches (Fig. 2c). Our calculations support the notion of a universal spin excitation spectrum at intermediate energies in the cuprates, arising from stripe-like charge-density fluctuations. This brings us closer to a unified description of the collective excitations in the high- T_c materials, and is applicable as well to other correlated oxides (nickelates, manganites) with tendencies towards stripe formation.

1. Rossat-Mignod, J. *et al.* Neutron scattering study of the $\text{YBa}_2\text{Cu}_3\text{O}_{6+x}$ system. *Physica C* **185–189**, 86–92 (1991).
2. Fong, H.-F. *et al.* Neutron scattering from magnetic excitations in $\text{Bi}_2\text{Sr}_2\text{CaCu}_2\text{O}_{8+\delta}$. *Nature* **398**, 588–591 (1999).
3. He, H. *et al.* Magnetic Resonant Mode in the Single-Layer High-Temperature Superconductor $\text{Tl}_2\text{Ba}_2\text{CuO}_{6+\delta}$. *Science* **295**, 1045–1047 (2002).
4. Tranquada, J. M. *et al.* Coexistence of, and Competition between, Superconductivity and Charge-Stripe Order in $\text{La}_{1.6-x}\text{Nd}_{0.4}\text{Sr}_x\text{CuO}_4$. *Phys. Rev. Lett.* **78**, 338–341 (1997).
5. Yamada, K. *et al.* Doping dependence of the spatially modulated dynamical spin correlations and the superconducting-transition temperature in $\text{La}_{2-x}\text{Sr}_x\text{CuO}_4$. *Phys. Rev. B* **57**, 6165–6172 (1998).

6. Mook, H. A., Dai, P., Dogan, F. & Hunt, R. D. One-dimensional nature of the magnetic fluctuations in $\text{YBa}_2\text{Cu}_3\text{O}_{6.6}$. *Nature* **404**, 729–731 (2000).
7. Emery, V. J., Kivelson, S. A. & Tranquada, J. M. Stripe phases in high-temperature superconductors. *Proc. Natl. Acad. Sci. USA* **96**, 8814 (1999).
8. Tranquada, J. M. *et al.* Quantum magnetic excitations from stripes in copper oxide superconductors. *Nature* **429**, 534–538 (2004).
9. Hinkov, V. *et al.* Two-dimensional geometry of spin excitations in the high-transition-temperature superconductor $\text{YBa}_2\text{Cu}_3\text{O}_{6+x}$. *Nature* **430**, 650–654 (2004).
10. Reznik, D. *et al.* Dispersion of Magnetic Excitations in Optimally Doped Superconducting $\text{YBa}_2\text{Cu}_3\text{O}_{6.95}$. *Phys. Rev. Lett.* **93**, 207003 (2004).
11. Hayden, S. M. *et al.* The structure of the high-energy spin excitations in a high-transition-temperature superconductor. *Nature* **429**, 531–534 (2004).
12. Stock, C. *et al.* From incommensurate to dispersive spin-fluctuations: The high-energy inelastic spectrum in superconducting $\text{YBa}_2\text{Cu}_3\text{O}_{6.5}$. *Phys. Rev. B* **57**, 024522 (2005).
13. Pailhes, S. *et al.* Resonant magnetic excitations at high energy in superconducting $\text{YBa}_2\text{Cu}_3\text{O}_{6.85}$. *Phys. Rev. Lett.* **93**, 167001 (2004).
14. Tranquada J. M. *et al.* Universal magnetic excitation spectrum in cuprates. Preprint at <<http://arxiv.org/pdf/cond-mat/0411082>> (2004).
15. Vershinin, M. *et al.* Local Ordering in the Pseudogap State of the High- T_c Superconductor $\text{Bi}_2\text{Sr}_2\text{CaCu}_2\text{O}_{8+\delta}$. *Science* **303**, 1995–1998 (2004).
16. Hanaguri, T. *et al.* A “checkerboard” electronic crystal state in lightly hole-doped $\text{Ca}_{2-x}\text{Na}_x\text{CuO}_2\text{Cl}_2$. *Nature* **430**, 1001–1005 (2004).
17. Batista, C. D., Ortiz, G. & Balatsky, A. V. Unified description of the resonance peak and incommensuration in high- T_c superconductors. *Phys. Rev. B* **64**, 172508 (2001).

18. Vojta, M. & Ulbricht, T. Magnetic excitations in a bond-centered stripe phase: Spin waves far from the semi-classical limit. *Phys. Rev. Lett.* **93**, 127002 (2004).
19. Uhrig, G. S., Schmidt, K. P. & Grüninger, M. Unifying Magnons and Triplons in Stripe-Ordered Cuprate Superconductors. *Phys. Rev. Lett.* **93**, 267003 (2004).
20. Manske, D., Eremin, I. & Bennemann, K. H. Analysis of the resonance peak and magnetic coherence seen in inelastic neutron scattering of cuprate superconductors: A consistent picture with tunneling and conductivity data. *Phys. Rev. B* **63**, 054517 (2001).
21. Eremin, I., Morr, D. K., Chubukov, A. V., Bennemann, K. H. & Norman, M. R. Novel neutron resonance mode in $d_{x^2-y^2}$ -wave superconductors. *Phys. Rev. Lett.* **94**, 147001 (2005).
22. Sachdev, S. Order and quantum phase transitions in the cuprate superconductors. *Rev. Mod. Phys.* **75**, 913 (2003).
23. Kivelson, S. A. *et al.* How to detect fluctuating stripes in the high-temperature superconductors. *Rev. Mod. Phys.* **75**, 1201 (2003).
24. Hasselmann, N., Castro Neto, A. H., Morais Smith, C. & Dimashko, Y. Striped phase in the presence of disorder and lattice potentials. *Phys. Rev. Lett.* **82**, 2135–2138 (1999).
25. Vojta, M. & Sachdev, S. Phenomenological lattice model for dynamic spin and charge fluctuations in the cuprates. Preprint at <<http://arxiv.org/pdf/cond-mat/0408461>> (2004).
26. Scalapino, D. J. & White, S. R. Numerical Results for the Hubbard Model: Implications for the High T_c Pairing Mechanism. *Foundations of Physics* **31**, 27–39 (2001).

27. Vojta, M. & Sachdev, S. Charge order, superconductivity, and a global phase diagram of doped antiferromagnets. *Phys. Rev. Lett.* **83**, 3916–3919 (1999).
28. Vojta, M. Superconducting charge-ordered states in cuprates. *Phys. Rev. B* **66**, 104505 (2002).
29. White, S. R. & Scalapino, D. J. Checkerboard patterns in the t - J model. *Phys. Rev. B* **70**, 220506(R) (2004).

Supplementary Information accompanies the paper on www.nature.com/nature.

Acknowledgements We thank A. V. Balatsky, W. Byers, B. Keimer, H. Mook, C. Pfleiderer, A. Rosch, J. Tranquada, and G. Uhrig for discussions, and especially S. Sachdev for collaborations on related work. This research was supported by the Virtual Quantum Phase Transitions Institute (Karlsruhe), by NSF Grants PHY99-0794 (KITP Santa Barbara), DMR-0339147 (TV), DMR-0103003 (RKK), the DAAD (RKK), and the Research Corporation (TV).

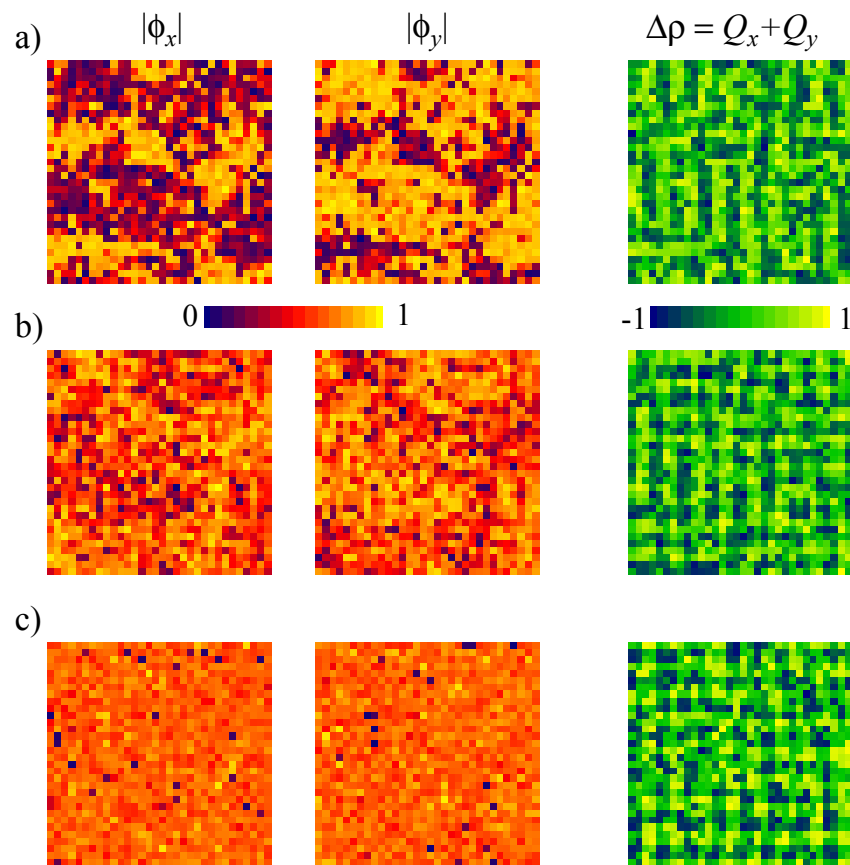
Competing Interests statement The authors declare that they have no competing financial interests.

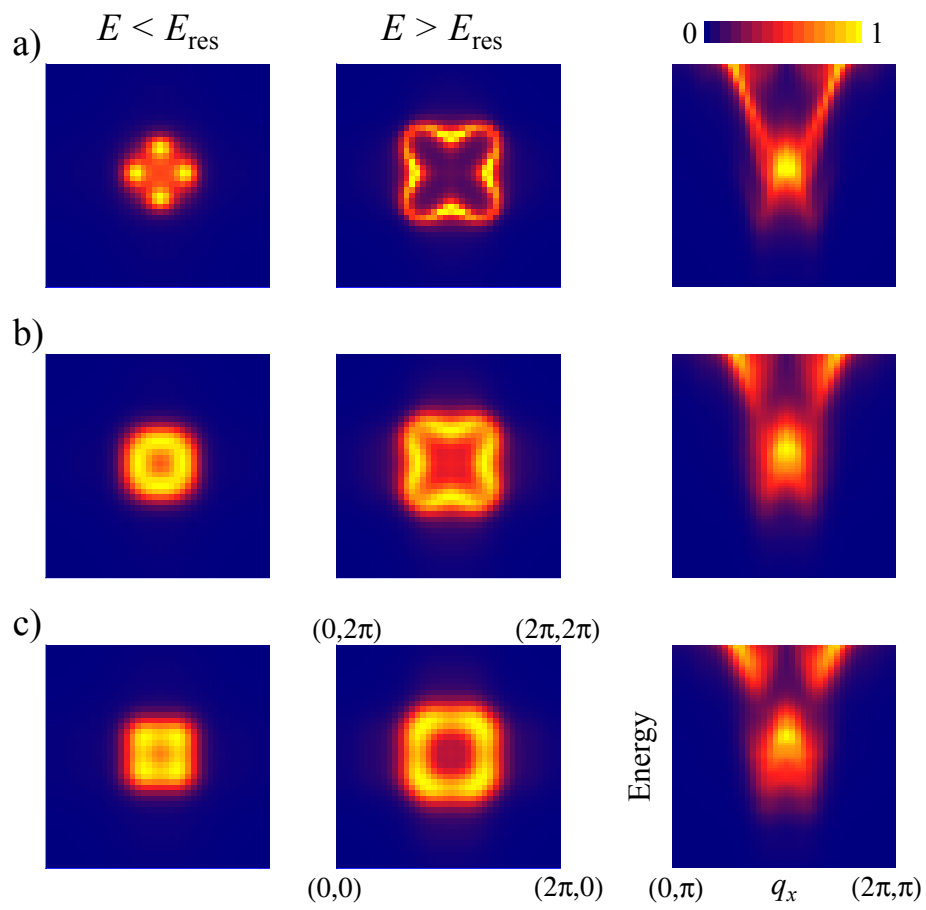
Correspondence and requests for materials should be addressed to M.V. (vojta@tkm.physik.uni-karlsruhe.de).

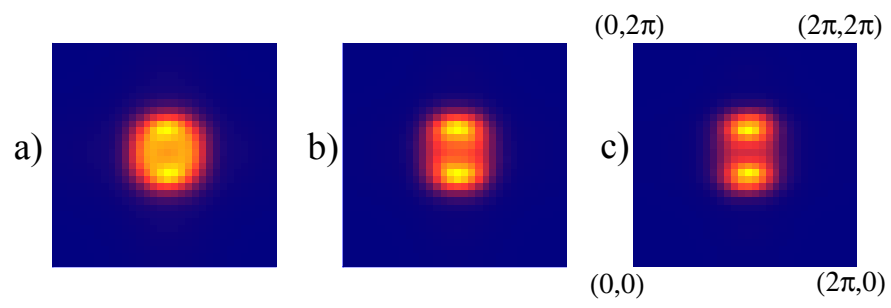
Figure 1 Monte-Carlo results for the charge sector, showing fluctuating stripes. Snapshots of the charge order parameters $\psi_{x,y}$ and the resulting charge modulation ($Q_x + Q_y$), obtained from MC simulations for bond-centered fluctuating stripes on 32^2 sites, using a ψ^6 action S_ψ , see Supplementary information. a) Strong repulsion between ψ_x and ψ_y , sharp domain walls. b) Weak repulsion, smooth domain walls with checkerboard structure. c) Weak attraction, fluctuating checkerboard order.

Figure 2 Spin excitation spectra in fluctuating stripe states. Dynamic susceptibility $\chi''(\mathbf{q}, \omega)$, as measured in inelastic neutron scattering, for bond-centered fluctuating stripes. Left/Middle: cuts at a constant energy, slightly below/above the resonance energy, E_{res} , as function of momentum. Right: cuts along (q_x, π) as function of q_x and energy, showing the universal “hour-glass” shaped spectrum. a) Strong repulsion between ψ_x and ψ_y , correlation length $\xi \approx 25$. b) Weak repulsion, $\xi \approx 20$. c) Weak attraction, $\xi \approx 20$.

Figure 3 Spin excitation spectra in the presence of a spatial anisotropy. Dynamic susceptibility, slightly below the resonance energy, for fluctuating stripes in the presence of an in-plane anisotropy. From a) to c) the anisotropy is increasing: the ratio of the gradient coefficients for $\psi_{x,y}$ in the charge action is a) 1.005, b) 1.01, c) 1.02.







Supplementary information for the paper:

Universal spin excitations in fluctuating stripe phases

Matthias Vojta, Thomas Vojta, and Ribhu K. Kaul

I. ORDER PARAMETER THEORY

Here we present the details of our phenomenological lattice order parameter theory, $\mathcal{S} = \mathcal{S}_\varphi + \mathcal{S}_\psi + \mathcal{S}_{x,y}$. The φ^4 theory for the spin sector assumes antiferromagnetic nearest-neighbor interaction on a square lattice and describes excitations near the *commensurate* wavevector $\mathbf{Q} = (\pi, \pi)$. Thus, the field φ is real and follows the quantum lattice action $\mathcal{S}_\varphi = \mathcal{S}_2 + \mathcal{S}_4$, with

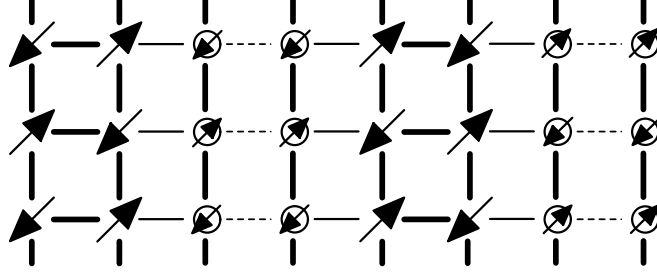
$$\mathcal{S}_2 = \int d\tau \sum_j \left[(\partial_\tau \varphi_j)^2 + s \varphi_j^2 \right] + \sum_{\langle jj' \rangle} c^2 (\varphi_j - \varphi_{j'})^2 \quad (1)$$

where $\langle jj' \rangle$ denotes a summation over pairs of nearest neighbor sites, and \mathcal{S}_4 is the quartic self-interaction term.

The two complex charge order parameter fields $\psi_{x,y}$ describe vertical and horizontal stripes, respectively. The resulting net modulation in the charge sector is $Q_x(\mathbf{r}) = \text{Re} \psi_x(\mathbf{r}) e^{i\mathbf{K}_x \cdot \mathbf{r}}$ (similarly for Q_y). Note that the $\psi_{x,y}$ and $Q_{x,y}$ fields are defined in the continuum, with $Q_x(\mathbf{r})$ for \mathbf{r} on sites measuring the modulation in the site charge density, whereas for \mathbf{r} on bonds $Q_x(\mathbf{r})$ refers to modulations in SU(2)-invariant bond variables like kinetic energy and pairing amplitude (representing bond order). We choose signs such that $\delta\rho(\mathbf{r}_j) = Q_x(\mathbf{r}_j) + Q_y(\mathbf{r}_j)$ is the deviation of the local *hole* density from its spatial average. The $Q_{x,y}$ fields are coupled to the spin sector by terms of the form $\lambda Q \varphi^2$ – these terms will cause the incommensurabilities in the spin susceptibility. Guided by the lattice models^{1,2} we choose³

$$\begin{aligned} \mathcal{S}_x = \int d\tau \sum_j & \left[\lambda_1 Q_x(\mathbf{r}_j) \varphi_j^2 + \lambda_2 Q_x(\mathbf{r}_{j+x/2}) \varphi_j \varphi_{j+x} \right. \\ & \left. + \lambda_3 Q_x(\mathbf{r}_j) \varphi_{j-x} \varphi_{j+x} + \lambda_4 Q_x(\mathbf{r}_{j+y/2}) \varphi_j \varphi_{j+y} \right], \end{aligned} \quad (2)$$

\mathcal{S}_y is obtained by $x \leftrightarrow y$. $\lambda_1 > 0$ implements the correlation between the on-site charge density and the amplitude of the spin fluctuations, while λ_{2-4} ensure that the effective



Supplementary Figure 1: Schematic illustration of the correlations between spin and charge order parameters, caused by λ_1 and λ_2 in the action \mathcal{S}_x , in a microscopic picture for a constant charge order parameter ψ_x . The arrows denote the spin order parameter on each site, with the arrow size being proportional to the spin amplitude. The circles indicate the hole density; for $\lambda_1 > 0$ large hole density is correlated with small spin amplitude. The lines refer to the magnetic interactions, thick/thin lines are for large/small antiferromagnetic couplings, whereas the dashed lines symbol ferromagnetic couplings. The λ_2 term in \mathcal{S}_x modulates the magnetic interaction according to the bond values of Q_x , as shown in the figure.

first- and second-neighbor exchange constants modulate along with the bond order, see Supplementary Fig. 1. In particular, the antiphase domain wall properties of the stripes^{4,5} are reflected in the positive sign of $\lambda_{2,3}$.

Now we turn to the model \mathcal{S}_ψ for the charge fluctuations. For slowly fluctuating charge order it is useful to think about snapshots of the charge configuration. Defining an $O(4)$ field $\psi = (\psi_x, \psi_y)$ we can discuss physically distinct spatial fluctuations: (i) Fluctuations of the complex phases of $\psi_{x,y}$ are stripe or checkerboard dislocations. (ii) Fluctuations between areas of dominant ψ_x or ψ_y represent domain walls between horizontal and vertical stripes. (iii) Variations in $|\psi|$ are amplitude fluctuations in the local charge order. Depending on the particular form of \mathcal{S}_ψ , these fluctuations will have different importance. Regarding amplitude fluctuations two extreme cases come to mind: (a) a standard ψ^4 theory with a “soft” order parameter, which has rather large amplitude fluctuations, and (b) a “hard” order parameter theory with a fixed-length constraint, $|\psi|^2 = \text{const}$. Although microscopically amplitude fluctuations are present, existing approximate results for Hubbard or t - J models are inconclusive with regard to their importance. Experimentally, STM results⁶ on $\text{Ca}_{2-x}\text{Na}_x\text{CuO}_2\text{Cl}_2$ indicate a spatially disordered arrangement of stripe segments and more

2d “tiles”, with the amplitude of these local modulations fluctuating rather little.

In our simulations, we have employed various forms for the charge action \mathcal{S}_ψ , with different amounts of amplitude fluctuations. Most useful is a ψ^4 -type theory for the O(4) field ψ , supplemented by a positive ψ^6 term:

$$\begin{aligned} \mathcal{S}_\psi = \int d\tau d^2\mathbf{r} & \left[|\partial_\tau \psi_x|^2 + |\partial_\tau \psi_y|^2 + c_{1x}^2 |\partial_x \psi_x|^2 + c_{2x}^2 |\partial_y \psi_x|^2 + c_{1y}^2 |\partial_y \psi_y|^2 + c_{2y}^2 |\partial_x \psi_y|^2 \right. \\ & + s_x |\psi_x|^2 + s_y |\psi_y|^2 + u_1 (|\psi_x|^2 + |\psi_y|^2)^2 + u_2 (|\psi_x|^2 + |\psi_y|^2)^3 + v |\psi_x|^2 |\psi_y|^2 \\ & \left. + w (\psi_x^4 + \psi_x^{*4} + \psi_y^4 + \psi_y^{*4}) \right]. \end{aligned} \quad (3)$$

A combination of $u_1 < 0$ and $u_2 > 0$ suppresses amplitude fluctuations of ψ . For $c_{1x} = c_{1y}$, $c_{2x} = c_{2y}$, $s_x = s_y$, and $v = w = 0$, the action has O(4) symmetry. The w term selects between bond-centered and site-centered stripes. The important quartic $v|\psi_x|^2|\psi_y|^2$ term regulates the repulsion or attraction between horizontal and vertical stripes, i.e., it determines whether the character of the order will be one-dimensional (stripe, for $v > 0$) or two-dimensional (checkerboard, for $v < 0$). We note that we have written down the action (3) in the continuum, as the ψ fields have distinct meaning on sites and bonds. In practice, we simulate \mathcal{S}_ψ on a square lattice, with discrete versions of the spatial derivatives, and interpolate for the bond values, e.g., $Q_x(\mathbf{r}_{j+x/2}) = [Q_x(\mathbf{r}_j) + Q_x(\mathbf{r}_{j+x})]/2$.

II. MONTE CARLO SIMULATIONS

Our adiabatic approximation assumes the fluctuations in the charge sector to be slow compared to those in the spin sector. Thus we generate a series of configurations of the charge fields $\psi_{x,y}$ by Monte Carlo simulations of \mathcal{S}_ψ (neglecting the feedback of the spins on the charges). For each configuration of the $\psi_{x,y}$, the remaining theory $\mathcal{S}_\varphi + \mathcal{S}_{x,y}$ (at the Gaussian level, $\mathcal{S}_4 = 0$) is quadratic in the φ fields and can be diagonalized on lattices up to 64^2 sites. (Neglecting \mathcal{S}_4 is justified in spin-disordered phases.)

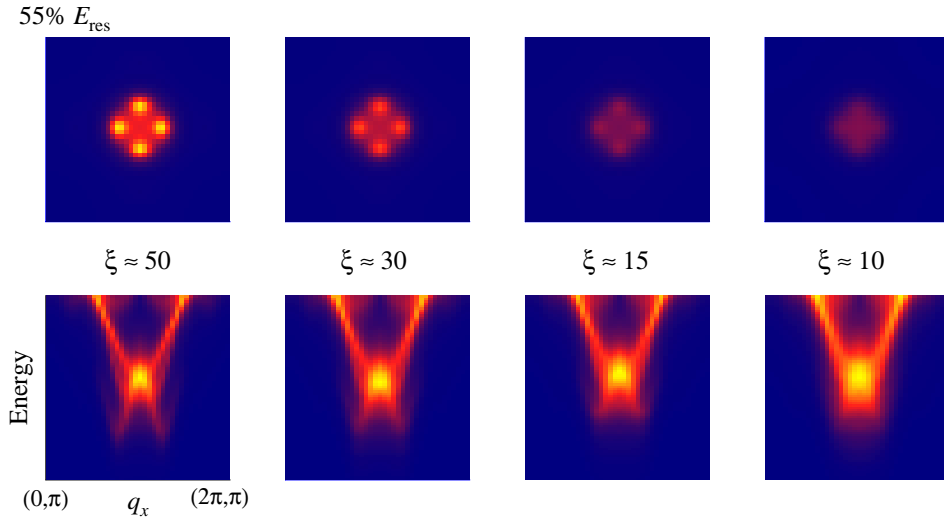
As details of the charge dynamics are unimportant for the resulting spin excitations, we replace the quantum dynamics in the charge sector by a classical one. We employ a standard Metropolis algorithm with single-site updates at a finite *effective* classical temperature to simulate \mathcal{S}_ψ in a regime where the correlation length ξ is between 5 and 50 lattice spacings. The spin susceptibility $\chi''(\mathbf{q}, \omega)$ is obtained by averaging its value over typically 20 MC charge configurations, with $10^5 - 10^6$ MC steps between two measurements.

III. PARAMETERS AND FURTHER RESULTS

The Monte Carlo simulations for the charge sector, \mathcal{S}_ψ , were performed at a classical temperature $T = 1$ – this sets a scale for all parameters in \mathcal{S}_ψ . The local parameters u_1 and u_2 in \mathcal{S}_ψ are chosen such that amplitude fluctuations are small near the phase transition; we have used $u_1 = -1 \dots -2$ and $u_2 = 0.1$. The velocities and mass terms are used to tune the correlation length, for the isotropic cases we had $c_{1x} = c_{1y} = c_{2x} = c_{2y} = 0.15 \dots 0.25$ and $s_x = s_y = -6 \dots -1$. The parameter v , selecting between stripes and checkerboard, was $v = 0.2, 0.04, -0.02$ for Fig. 2a,b,c, respectively. Finally, we employed $w = 0.05$ resulting in bond-centered stripes. Simulations with site-centered stripes yielded qualitatively similar results, but we found that in this case charge fluctuations are more effective in destroying the incommensurate spin correlations, i.e., the charge correlation length necessary to obtain a well-defined downward dispersing branch in the susceptibility, $\chi''(\mathbf{q}, \omega)$, is significantly larger than for bond-centered stripes.

The above parameters fix a typical order parameter amplitude $|\psi|_{\text{typ}}$. (Note that no connection to the absolute microscopic charge modulation can be made in this phenomenological approach. Therefore, the normalization of $\psi_{x,y}$ and $Q_x + Q_y$, e.g. in Fig. 1, is arbitrary.) In the spin action, \mathcal{S}_φ , the velocity c sets the spin energy scale – this can be connected to experiment, resulting in $c \approx 100$ meV. The parameter s in \mathcal{S}_φ tunes the “bare” spin gap (which is different from the true spin gap due to the coupling to the charge sector). For the coupling between spin and charge sectors, $\mathcal{S}_{x,y}$, only the product $\lambda|\psi|_{\text{typ}}$ enters. We have chosen s and the λ such that a fluctuationless charge-ordered reference state has gapless incommensurate spin excitations as in Ref. 3. With $c = 100$ meV we obtain $E_{\text{res}} \approx 40$ meV, where E_{res} is defined by the intensity maximum of $\chi''(\mathbf{q}, \omega)$ at $\mathbf{q} = (\pi, \pi)$. In Fig. 2 we have used $\lambda_1 = \lambda_3/2 = 5E_{\text{res}}/|\psi|_{\text{typ}}$, $\lambda_2 = \lambda_4 = 0$. The in-plane anisotropy in Fig. 3 is implemented via $c_{1x} = c_{2x}$, $c_{1y} = c_{2y}$ with $c_{1x}/c_{1y} \neq 1$ as quoted in the figure caption.

In the Supplementary Fig. 2 we report our results for the dynamical spin susceptibility in a stripy situation, as in Figs. 1a, 2a, as function of the charge correlation length ξ . The downward dispersing lower branch is most pronounced for well-defined stripes, i.e., large ξ ; it is progressively smeared out with decreasing ξ . Experimentally, the charge correlation length will vary as a function of both doping level and temperature, with ξ being larger in the underdoped regime at low temperatures. In this context we note that very recent



Supplementary Figure 2: Evolution of the dynamic spin susceptibility, $\chi''(\mathbf{q}, \omega)$, with increasing stripe correlation length ξ , for a situation with strong repulsion between ψ_x and ψ_y . The top panel shows constant-energy scans at 55% of the resonance peak energy E_{res} , the bottom panel shows cuts along (q_x, π) as function of q_x and energy. The incommensurate spin response in the lower branch is most pronounced for large ξ , resulting in an “hour-glass” or “X”-shaped spectrum. In contrast, small ξ smears the resonance peak and yields a more “Y”-shaped spectrum with little momentum dependence over a significant energy range around E_{res} .

neutron scattering results⁷ indicate a “Y”-shaped response in the pseudogap state above T_c in underdoped YBCO_{6.6}, with little dispersion at low energies. We conclude that these data, which are very similar to our results in the right panel of the Supplementary Fig. 2, are consistent with fluctuating short-range stripe segments.

-
- ¹ Vojta, M. & Ulbricht, T. Magnetic excitations in a bond-centered stripe phase: Spin waves far from the semi-classical limit. *Phys. Rev. Lett.* **93**, 127002 (2004).
 - ² Uhrig, G. S., Schmidt, K. P. & Grüninger, M. Unifying Magnons and Triplons in Stripe-Ordered Cuprate Superconductors. *Phys. Rev. Lett.* **93**, 183004 (2004).
 - ³ Vojta, M. & Sachdev, S. Phenomenological lattice model for dynamic spin and charge fluctuations in the cuprates. Preprint at <http://arxiv.org/pdf/cond-mat/0408461> (2004).
 - ⁴ Emery, V. J., Kivelson, S. A. & Tranquada, J. M. Stripe phases in high-temperature supercon-

- ductors. *Proc. Natl. Acad. Sci. USA* **96**, 8814 (1999).
- ⁵ Scalapino, D. J. & White, S. R. Numerical Results for the Hubbard Model: Implications for the High Tc Pairing Mechanism. *Foundations of Physics* **31**, 27-39 (2001).
- ⁶ Hanaguri, T. *et al.* A “checkerboard” electronic crystal state in lightly hole-doped $\text{Ca}_{2-x}\text{Na}_x\text{CuO}_2\text{Cl}_2$. *Nature* **430**, 1001-1005 (2004).
- ⁷ Hinkov, V. *et al.* In-plane anisotropy of spin excitations in the normal and superconducting states of underdoped $\text{YBa}_2\text{Cu}_3\text{O}_{6+x}$. Preprint at <http://arxiv.org/pdf/cond-mat/0601048> (2006).